Magazine of Civil Engineering

ISSN 2071-0305

journal homepage: http://engstroy.spbstu.ru/

DOI: 10.18720/MCE.95.1

Seismic design philosophy of special steel plate shear walls

P. Ebadi*, S. Farajloomanesh

Department of Civil Engineering, Shahr-e-Qods Branch, Islamic Azad University, Tehran, Iran

** E-mail: parviz.ebadi@gmail.com*

Keywords: seismic, steel plate shear wall, capacity design, optimization, ductility

Abstract. Steel plate shear walls are usually designed by devoting total story shear to plates and designing peripheral frames for total transferred forces from the plates to the peripheral frames. Therefore, the participation of frames in the story shear neglected conservatively. In this research, a design methodology is presented based on the real sharing of steel walls and peripheral frames in story shear. Steel walls are designed using Plate-Frame Interaction (PFI) theory for different percentages of story shear and their seismic parameters compared together by numerical modeling in nonlinear analysis software. The obtained results indicated that using the conventional design methods, devoting total story shear to the steel walls and neglecting the shear capacity of the peripheral frame could lead to the over-designed (conservative) sections. In contrast, if the seismic design of this system was performed considering the sum of the capacity of steel plate and peripheral frame and their real sharing in story shear, the system design would be efficient and economical.

1. Introduction

Numerous studies have been conducted on Steel Plate Shear Walls (SPSW) in recent years. Roberts and Sabouri-Ghomi [1] tested 16 steel shear panels at the University of Wales and showed that all the panels had sufficient ductility during large inelastic cycles. The Plate-Frame Interaction (PFI) theory introduced for analyzing SPSW with and without stiffener and opening [1, 2]. In this theory, the behavior of the frame and plate are investigated independently and their interactions are taken into consideration. Gholhaki [3] tested two specimens of SPSW with hinge and rigid connections for end of beams and found that the effect of the beam-column connection type on the initial stiffness of the walls could be ignored. But, the strength of the specimen with rigid connection was higher than that of the hinge one by almost 26 percent. Furthermore, the energy absorption capacity of the specimen with rigid connection was higher than that of the specimen with hinge connection. Moreover, the effect of the beam-column connection on the angle of the diagonal tension field was insignificant. Darvishi et al. [4] tested three models with the panel width-to-height ratio of smaller than 1, equal to 1, and higher than 1 and concluded that, in the first case, the increased stiffness of the column increased the ductility of the overall structure as well as the over-strength factor. In the second case, had no significant effect, while in the third case, reduced ductility and over-strength factor. Based on the studies conducted by Alinia and Dastfan [5–7] on SPSW, it can be concluded that high energy absorption of the steel shear wall system depends on the stiffness of the boundary elements. Several laboratory studies were conducted at the laboratory of Assessment and Planning Center of Construction and Transportation Industry in South Korea in order to investigate the bearing capacity variations of the shear walls made of steel plates with various construction details [8]. Kharrazi et al. [9] proposed the Modified Plate-Frame Interaction (M-PFI) theory, in which the effect of -bending on the SPSW system response was taken into account in the load-displacement diagram. Chen and Jhang [10] examined the effect of using steel with Low Yield Point (LYP) on designing steel shear walls and demonstrated that limiting the plate's width-to-thickness ratio to below 80 would improve the wall's performance. In addition, the use of beam-column moment connection, instead of shear connection, would increase the system's strength and energy dissipation capacity by 28 % and 18 %, respectively. Hosseinzadeh and Tehranizadeh [11] studied SPSW with different stories and width-to-height ratios. They concluded that the plate yield in the panels with a smaller number of stories would occur greatly earlier than the peripheral frame, while in the case of more number of stories, the full yield of plates would be

postponed. Furthermore, since the steel walls could only work in tension, not compression, the axial tensile forces in the columns would be less than their axial compressive forces. Moradinejad et al. [12] investigated the effect of the location of the SPSW on progressive collapse. The results of the nonlinear static analyses showed that the location of SPSW at the corner of the plan improved the structure's behavior against the progressive collapse. Ebadi et al. [13, 14] examined the effect of the steel wall contribution to the lateral load transfer and represented that the more the plate's contribution to the lateral load, the more the thickness of the plate and the more non-economic and conservative design of the structure would be. Purba and Bruneau [15] tested a 1/3-scale model of three-story SPSW specimen and suggested that development of in-span hinges should be explicitly avoided in the design of Horizontal Boundary Elements (HBE) and mentioned that, in some instances, the ordinary-type connection specified by the code to be used in SPSWs might not be sufficient to sustain large rotation demand that could occur in the connections. Moghimi and Driver [16] studied performance of SPSW under accidental blast loads and found that despite the inherent slenderness of the steel members, the SPSW system would be an effective potential protective structure in industrial plants. The side wall subjected to in-plane blast load is a strong and reliable system, and the front wall subjected to out-of-plane blast load can be sized to provide acceptable design for industrial plant applications. Guo et al. [17] studied the influence of hinged, rigid and semi-rigid beam-column connection types on the behavior of SPSW structures. They concluded that the semi-rigid composite frame with SPSW is an effective lateral load resisting system. So that, the semi-rigid frame and the shear wall work together to satisfy higher safety margins.

Du et al [18] made Pseudo-static test on SPSW specimen and studied method of anchoring stiffeners to the steel plate to reinforce the structure.

Wang et al [19] observed that the lateral stiffness and bearing capacity of horizontal corrugated SPSWs are higher than those of vertical corrugated SPSWs, in contrast to the case of corrugated steel plate reinforced concrete composite shear walls.

Jalali and Darvishan [20] enhanced modelling of self-centering steel plate shear walls. They used a set of 44 earthquake ground motions by comparative nonlinear response history analyses.

Yu et al [21] investigated SPSWs with different types of stiffener and found that the performance of SPSWs enhanced by using multiple ribs and precast concrete panel. In addition, out-of-plane deformation of plate decreased by increasing restraining stiffness.

Pachideh et al [22] analyzed 27 frames, including 18 frames with thin steel plate shear walls, as lateral load resisting system along with 9 special moment-resisting frames with three different heights in short, intermediate and tall configurations. The observations demonstrated that the damage index for SPSW in taller frames led to better results and higher safety compared to other frames.

Hajimirsadeghi et al [23] conducted a full scale cyclic experiment on an enhanced modular shear wall SPSW and continued up to fail. Test results revealed high initial stiffness, excellent ductility, and significant energy dissipation capacity of the system.

Mu and Yang [24] proposed SPSWs with oblique channel-shaped stiffeners. They studied Seismic behaviors of obliquely stiffened SPSWs with openings. They observed that the multi-oblique stiffening form could effectively improve the buckling load of plates and delay the formation of tension field.

In Seismic Provisions for Structural Steel Buildings [25] and Steel Plate Shear Wall Design Guide [26], the design of the beams and columns depends on tension field forces resulted from the plates. In other words, the increased thickness of the steel plate would lead to the increased transitional force caused by the plate's tension field on the wall's boundary elements, resulting in the increased size of the columns. In the conventional design methods for steel walls, the steel plate is designed for the total story shear and the effect of the frame on the story shear is ignored, while the peripheral frame can transfer a considerable lateral force. Thus, it is expected that assigning total story shear to the plate would increase the thickness of the plate, imposes additional forces to the beams and columns, and finally, leads to the over-designed (conservative) sections of the beams and columns.

In this paper, in order to evaluate the lateral load bearing capacity of stories in conventional design methods, a 10-story steel building designed. Then, the sketched PFI diagrams for different stories indicated much higher capacity of each story relative to the required story shear. Afterwards, a repetitive trial-and-error design philosophy was proposed by precisely determining the contribution of the steel plate and its' peripheral frame to the total story shear of SPSW. At the next stage, in order to examine the effect of the contribution of the wall and frame to the story shear, the steel walls and peripheral frames re-designed for 75 % and 50 % of the demand story shear. Therefore, the transferred tension field forces from the steel wall to peripheral frame decreased. At the final stage and according to the proposed design method, the actual contribution of the steel walls to the story shear was calculated and the optimal design contributions was presented. PFI diagrams sketched for all the specimens and the seismic parameters of the frames, including ductility, response modification factor, over-strength factor, and energy absorption capacity were calculated.

2. Methods

2.1. Plate-Frame Interaction (PFI) theory

The PFI theory is one of the most powerful tools for calculating the capacity of SPSW. Thus, it was used to evaluate the capacity of the studied frames. In PFI theory, the capacity diagrams of the frame and plate are evaluated separately, and the capacity of SPSW is calculated by summing up the capacity diagrams of the plate and frame. PFI parameters for the frame are defined in Fig. 1.

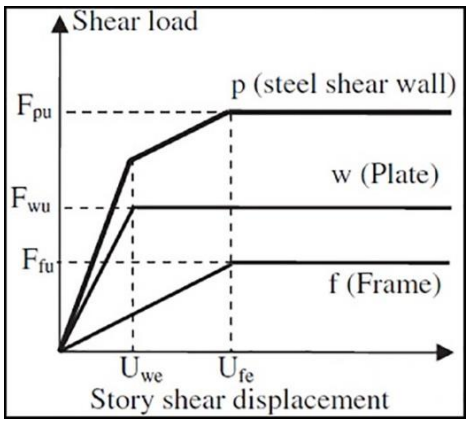

Figure 1. PFI parameters [1].

Where F_{wu} is the ultimate shear strength of plate, U_{we} is the shear yield displacement of the plate, F_{fu} is the ultimate shear strength of the frame, and U_{fe} is shear yield displacement of the frame, calculated using Eq (1–4).

$$F_{wu} = b.t\left(\tau_{cr} + 0.5\sigma_y \sin 2\theta\right) \tag{1}$$

$$U_{we} = \frac{2\sigma_y}{E \sin 2\theta} d \tag{2}$$

$$F_{fu} = \frac{4M_{fp}}{d} \tag{3}$$

$$U_{fe} = \frac{M_{fp} d^2}{6EI_f} \tag{4}$$

Where b and d indicate the panel's width and height, respectively, t is the plate's thickness, E is the steel plate modulus of elasticity, σ_y is the uniaxial yield stress of the steel plate, τ_{cr} is the plate's critical shear stress, and θ is the angle of tension field inclined respect to the horizontal line, M_{fp} is the plastic moment of columns, I_f is the moment of inertia of columns, F_{fu} and F_{wu} are shear capacity of peripheral frame and steel plate, respectively, and U_{wf} and U_{we} are lateral yield displacement of peripheral frame and steel plate, respectively.

The system's total capacity (F_{pu}) is calculated by Eq (5).

$$F_{pu} = F_{fu} + F_{wu} \tag{5}$$

2.2. Optimal design of SPSW

In the conventional design method of SPSWs, total story shear is allocated in the wall. Therefore, the peripheral frame's contribution to the story shear is neglected conservatively.

However, in the optimal design of the SPSW, which was investigated in this paper, the lateral load capacity of the peripheral frame is also considered. In other words, the trial-and-error method implemented to determine the actual contribution of the steel wall and peripheral frame in the story shear. It should be noted that the contribution of steel wall and frame is not constant on all the stories. Accordingly, since the dimensions of the lower columns

depend on the thickness of the steel wall in the upper stories, it is necessary to start the optimization from the highest stories and, eventually, end it on the ground story.

According to Clause-17.2 of AISC341 [25], the nominal shear strength for the SPSW is calculated by Eq (6).

$$V_n = \varphi \times 0.42 \times F_y \times L_{cf} \times t_w \times \sin 2\alpha \quad (6)$$

Where φ is the strength reduction factor and is equal to 0.9, F_y, L_{cf}, t_w, and α indicate specified minimum yield-stress of steel, clear distance between columns, steel wall thickness, and angle formed by tension field on the vertical wall, respectively.

According to PFI equations, the shear strength and displacement corresponding to the plate, frame, and panel are obtained by Eq (1–4).

AISC has considered the ratio of the expected tensile strength to the specified minimum tensile strength ($R_t = 1.2$) in Eq (6); in other words, being divided by 1.2. Therefore, the coefficient of 0.5 in Eq (1) from PFI theory has been changed to 0.42 in Eq (6) from AISC341 (0.5/1.2= 0.42). Furthermore, the plate's critical shear stress (τ_{cr}) is insignificant in Eq (1), which has been neglected in AISC equations. Thus, if Eq (1) is multiplied by (φ/1.2)=(0.9/1.2)=0.75 and also τ_{cr} = 0 is taken into account, Eq (1) and (6) will be equivalent.

Since the AISC load method and ultimate strength have been used in designing the wall, it is necessary to apply the following changes for drawing the PFI diagrams:

$$\frac{0.9}{1.2}(PFI) \approx V_{demand} \quad (7)$$

Where V_{demand} is the design base shear from building code. In other words, Eq (7) can be rewritten as follows:

$$F_{pu} = F_{wu} + F_{fu} = 1.33 \times V_{demand} \quad (8)$$

Thus, in order to use PFI in design, demand shear (V_{demand}) should be multiplied by 1.33 and the steel wall and frame must be designed such that their total capacity exceeds the required base shear of the story by 1.33 times.

The process of the optimal design of the SPSW is as follows:

1. Optimization is started from the highest story and ends on the ground story.

2. Assumption of the certain percentage of the plate and frame sharing on each story shear is considered.

3. Thickness of the steel wall is determined by Equations (6), (7), and (8).

4. The maximum force transferred from the steel wall to the peripheral frame is determined and combined with gravitational loads.

5. Frames are designed for the applied loads in Step 4.

6. The capacity of the frame and wall is calculated and compared with the story's required base shear.

7. If the calculated capacity in Step 6 is higher than the story's required capacity, the wall thickness must be reduced and steps 2–6 must be repeated; however, if the capacity is less, thickness of the wall must be increased and the aforementioned steps must be repeated.

8. After optimizing the story, the optimization process is carried out for the lower stories, respectively. It should be noticed that the forces of the upper stories are transferred to the lower stories after optimization.

2.3. Design of frames

The studied building was a 10-story residential building with local soil type 3 (shear wave velocity of 175~375 m/s), story height of 3 meters and located in a high seismic hazard zone. Plans of the stories are shown in Fig. 2 and the steel walls were located around the plan. By assuming the uniform lateral load distribution according to the structure's weight on each wall, only a part of the structure plan with the affected weight for design of one of the walls is shown in Fig. 2.

The materials of the SPSW were of the S235J type with the minimum yield strength of 235 MPa and materials of the beams and columns were of the S350J type with the minimum yield strength of 350 MPa. Dead load of the stories and roof, live load of the stories, and live load of the roof were equal to 5, 2, and 1.5 kN/m^2, respectively. Structural response modification factor was considered equal to 7 in accordance with Minimum Design Loads for Buildings and Other Structures (ASCE7-10) [27]. Cross-section of the columns was considered as a hollow square section; besides, to ensure the plastic hinge in the beams (strong column-weak beam principle), the beam-column connection of RBS[1] type was used. The SPSW was designed based on the requirements of Seismic Provisions for Structural Steel Buildings (AISC 341) [25] and AISC Design Guide 20 [26] using Load and Resistance Factor Design (LRFD) method.

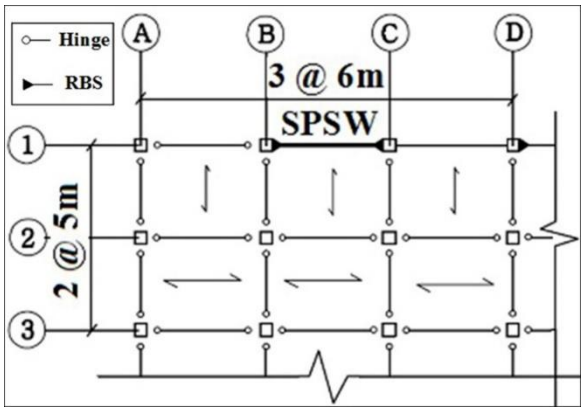

Figure 2. Plan of buildings.

The studied frames were named as SPSW-xx, where xx indicate the portion of the total shear load of the story (in percent), which was used for the wall design and was selected equal to 50, 75, and 100 percent. The optimal design was also shown by "opt" symbol. Furthermore, in order to prevent increased seismic demand of the system, the computational thickness was used for the steel walls.

In Table 1, the wall's contribution to the lateral load transfer is specified for four studied specimens on various stories. It can be seen that in the optimal design, the plate's contribution to the system shear strength was much less than the conventional design method, which is on average about 33 % (instead of 100 %). In addition, on the highest story, the contribution of the plate was reduced compared to other stories, which was due to using larger dimensions for columns because of executive problems. According to Table 1, by reducing the plate's contribution to the story shear, the thickness of the plate and dimensions of the boundary elements reduced. As will be discussed in the following sections, the system's capacity in specimens SPSW-100, SPSW-75, and SPSW-50 was still higher than the story shear, while in the optimal frame, the capacity of the system became equal to the structural story shear demand.

In Table 2, the designed sections of the frame on axis 1 between axes B and C are shown (see Fig. 2). The designed sections were named based on the nominal dimensions and the thicknesses of the sections. For instance, in the third column of this Table, B360x25 refers to the Hollow Square Section (HSS) with outside dimension of 360 mm and thickness of 25 mm. In addition, in the fourth column, b600x-310x-25x-12 indicates the plate girder with the height of 600 mm, flange width of 310 mm, flange thickness of 25 mm, and web thickness of 12 mm.

Table 1. Percentage of the plate's contribution in shear strength of each story.

Story	SPSW-100	SPSW-75	SPSW-50	SPSW-Opt
	Percentage of the Plate's Contribution (%)			
10	100	75	50	13
9				28
8				34
7				38
6				34
5				33
4				33
3				33
2				32
1				34

[1] Reduced Beam Section

Table 2. Design sections of frames*.

Story	Plate Thickness	Column	Beam	Story	Plate Thickness	Column	Beam
SPSW-100				SPSW-75			
10	1	B360x25	b600x-310x-25x-12	10	0.8	B300x25	b600x-220x-25x-10
9	2	B360x25	b600x-310x-25x-12	9	1.5	B300x25	b600x-250x-20x-10
8	2.8	B400x30	b600x-310x-25x-12	8	2.1	B350x30	b600x-250x-20x-10
7	3.6	B400x30	b550x-280x-25x-10	7	2.7	B350x30	b550x-250x-20x-10
6	4.2	B450x35	b550x-280x-25x-10	6	3.1	B400x30	b550x-250x-20x-10
5	4.7	B450x35	b550x-220x-20x-10	5	3.5	B400x30	b450x-260x-20x-8
4	5.2	B500x35	b550x-220x-20x-10	4	3.9	B450x35	b450x-260x-20x-8
3	5.5	B500x35	b450x-210x-20x-10	3	4.1	B450x35	b400x-190x-20x-8
2	5.7	B550x40	b450x-210x-20x-10	2	4.2	B500x35	b400x-190x-20x-8
1	5.8	B550x40	b450x-150x-20x-10	1	4.3	B500x35	b400x-190x-20x-8
SPSW-50				SPSW-Opt			
10	0.5	B250x20	b550x-210x-20x-10	10	0.1	B210x20	b350x-200x-20x-6
9	1	B300x25	b550x-210x-20x-10	9	0.5	B260x20	b450x-280x-20x-8
8	1.4	B300x25	b450x-280x-20x-10	8	0.9	B290x20	b450x-280x-20x-8
7	1.8	B340x30	b450x-280x-20x-10	7	1.3	B290x25	b450x-280x-20x-8
6	2.1	B340x30	b450x-280x-20x-10	6	1.4	B320x25	b450x-240x-20x-8
5	2.3	B340x30	b400x-220x-20x-8	5	1.5	B320x30	b450x-240x-20x-8
4	2.5	B360x30	b400x-220x-20x-8	4	1.7	B330x30	b450x-240x-20x-8
3	2.7	B360x30	b350x-200x-20x-8	3	1.8	B340x30	b450x-240x-20x-8
2	2.8	B410x35	b350x-200x-20x-8	2	1.8	B350x30	b400x-150x-15x-8
1	2.9	B410x35	b350x-180x-15x-8	1	1.9	B360x30	b400x-150x-15x-8

* All dimensions are in mm.

3. Results and Discussion

3.1. Force-displacement diagrams

3.1.1. First story

Force-displacement diagrams of the first, fifth, and tenth stories for the studied panels are shown in Figures 3 to 5. Diagrams of the other stories and system behavior were the same and neglected in order to summarize the paper. In these diagrams, the PFI theory is used, where P, F, and W indicate Panel, Frame, and Wall, respectively. Therefore, the total capacity of the structure in SPSW-100 in Fig. 3a was almost 3 times as the required shear capacity of the story.

In Fig. 3b and 3c, in which the plates were designed for 75 % and 50 % of the story shear, the total capacity of the structure was obtained equal to 8482 and 4989 kN, which was 2.3 and 1.3 times as the story's shear demand (equal to 3681 kN), respectively. In Fig. 3d, the optimal value for the plate's shear sharing (equal to 34 %) is calculated using the trial-and-error method. Besides, the total capacity of the structure in SPSW-100 was 1.3 times of SPSW-75. It is also 2.3 and 3 times of SPSW-50 and SPSW-Opt specimens, respectively. As shown in Fig. 3d, the total capacity of the structure was equal to the story's shear demand.

Panel's stiffness in SPSW-100 was 1.4, 2.8, and 4 times as those of SPSW-75, SPSW-50, and SPSW-Opt specimens, respectively. The plate-to-frame initial stiffness ratio in SPSW-75, SPSW-50, and SPSW-Opt was equal to 0.7, 0.8, and 1.1, respectively.

As observed, the less the wall plate contribution to the story shear capacity, the smaller the peripheral frame and the higher the yield deformation of the frames would be. Therefore, by increasing the distance between the yield deformations of the frame and wall, the system's energy absorption capacity would be increased as well. It is also notable that by allocating the whole story shear to the steel wall, the frame's initial stiffness in Fig. 3a was more than that of the wall, and the dominant behavior of the system would be the peripheral frame.

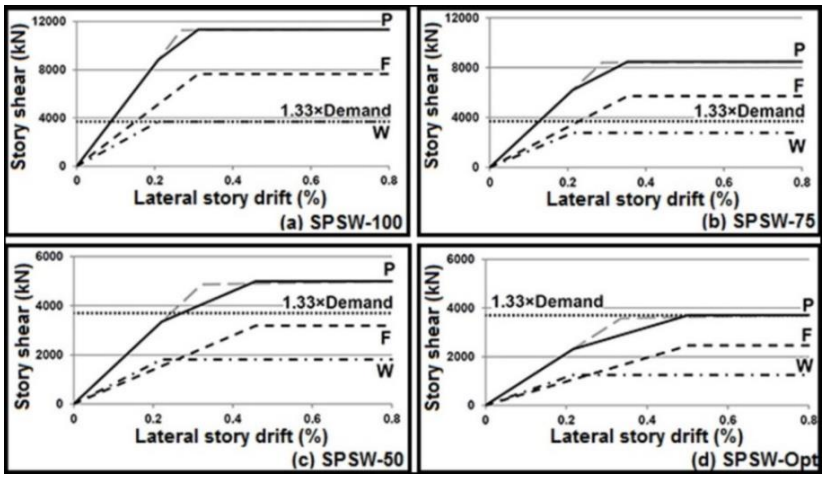

Figure 3. PFI diagram of the first story and comparison with design story shear demand; a) SPSW-100, b) SPSW-75, c) SPSW-50, d) SPSW-Opt.

3.1.2. Fifth story

In order to summarize the results, some stories investigated as a sample. In this section, the results for the fifth story are discussed. Force-displacement diagram of the fifth story for the studied frames is shown in Fig. 4. According to Fig. 4a, the total capacity of the structure was 2.6 times of the story's shear demand. It indicates that the design of steel wall for the total base shear of the story and neglecting the bearing capacity of the peripheral frame leads to over-design procedure. In Fig. 4b and 4c, the total capacity of the structure was obtained equal to 5706 and 3884 kN, which was 1.8 and 1.3 times of the story's demand shear (equal to 3053 kN), respectively. The percentage of the plate's contribution to the fifth story of the optimum specimen was calculated as 33 percent.

Panel stiffness on the fifth story in SPSW-100 was 1.5 times of that in SPSW-75, and 2.5 and 3.5 times of SPSW-50 and SPSW-Opt, respectively. The total capacity of the structure in SPSW-100 was 1.4, 2.1, and 2.6 times of those in SPSW-75, SPSW-50, and SPSW-Opt, respectively. The plate-frame stiffness ratio in SPSW-100 was equal to 1. Furthermore, in SPSW-75, SPSW-50, and SPSW-Opt specimens, it was equal to 1.2, 1.4, and 1.1, respectively.

Frame-to-plate yield stress ratio in SPSW-100, SPSW-75, SPSW-50, and SPSW-Opt specimens was equal to 1.7, 1.9, 2.2, and 2.4, respectively. In other words, by reducing the wall's contribution to the story shear, this ratio was increased, which was consistent with the philosophy of the peripheral frame contribution in the story shear.

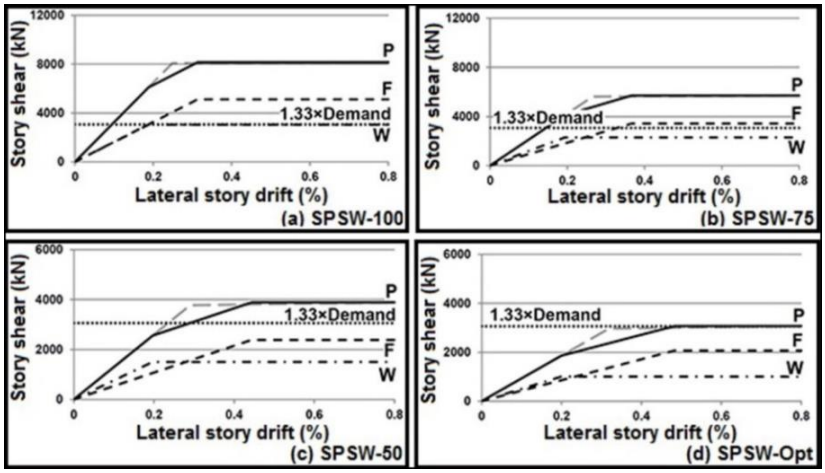

Figure 4. PFI diagram of the fifth story and comparison with design story shear demand; a) SPSW-100, b) SPSW-75, c) SPSW-50, d) SPSW-Opt.

3.1.3. Tenth story

Force-displacement diagrams of the tenth story for the studied specimens are shown in Fig. 5. Total capacity of the structure in Fig. 5a was 4.7 times of the demand shear capacity of the story. In Fig. 5b and 5c, the structure's total capacity was obtained as 2185 and 1244 kN, which was 3.2 and 1.8 times of the demand

shear capacity of the story (681 kN), respectively. In Fig. 5d, the percentage of the plate's optimal contribution to the story shear was calculated equal to 13 percent. Panel stiffness in SPSW-100 was 1.7, 3.3, and 9.1 times of the ones in SPSW-75, SPSW-50, and SPSW-Opt, respectively. Furthermore, the structure's total capacity in SPSW-100 was 1.5, 2.6, and 4.7 times of the ones in SPSW-75, SPSW-50, and SPSW-Opt, respectively.

The plate-to-frame stiffness ratio in SPSW-100, SPSW-75, SPSW-50, and SPSW-Opt was 0.4, 0.7, 1, and 0.5, respectively. As expected, by reducing the plate's contribution to the lateral load, the plate-to-frame stiffness ratio was increased. The reduction in the plate-to-frame stiffness ratio in SPSW-Opt was due to the application of executive limitations on the minimum dimension size of the columns in 10th story as well as the plate's low contribution (13 %) to the panel shear strength. The frame-to-plate yield stress ratio in SPSW-100, SPSW-75, SPSW-50, and SPSW-Opt was 1.9, 2.3, 2.9, and 3.7, respectively.

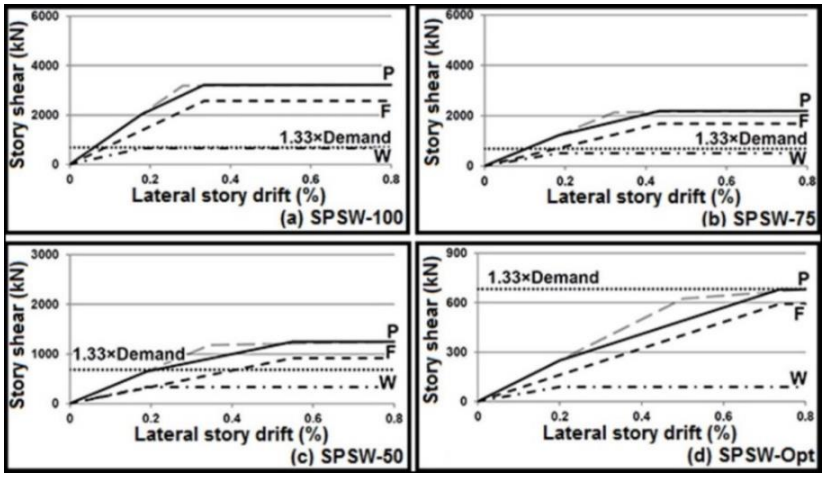

Figure 5. PFI diagram of the tenth story and comparison with design story shear demand; a) SPSW-100, b) SPSW-75, c) SPSW-50, d) SPSW-Opt.

3.1.4. Comparison of the design methods

Fig. 6 represents the comparison between the panel force-displacement diagrams on the studied sorties. It can be seen that by reducing the wall's contribution to the story shear capacity, the stiffness of the panel reduced. Moreover, the system's capacity in the optimum specimen (SPSW-Opt) was equalized with the demand story shear. Interestingly, in the studied diagrams, the steel plate's yield displacement was almost constant, while the yield displacement of the frame was increased. In other words, the increase in the distance between the yield displacement of the steel plate and frame led to the increased energy absorption capacity in this region. Details of the calculations of these displacements on different stories of the studied specimens are presented in Table 3.

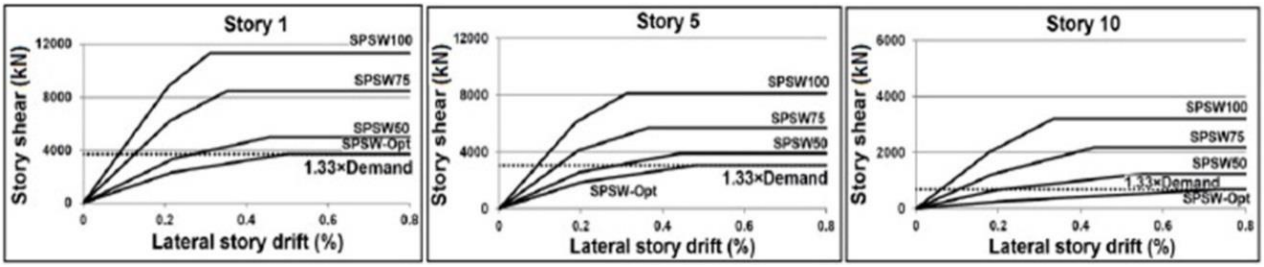

Figure 6. Comparing panel force-displacement diagrams in the studied specimens.

As seen in Table 3, owing to the 25 % reduction in the plate's contribution to the lateral load, the average plate yield displacement (U_{we}) and average frame yield displacement (U_{fe}) were increased by 3 % and 20 %, respectively.

Regarding the investigation of the PFI diagrams on the stories of the structure, in contrast to the conventional conservative design method, shear capacity of the frame was much higher than that of the steel plate. In other words, the plate's contribution to the story shear was less than the peripheral frame and neglecting the frame shear capacity in calculations might result in the overdesigned sections. It should be noted that the lateral stiffness of the frame was also higher than that of the steel plate.

Table 1. Plate-frame yield displacement in PFI diagrams*.

Story	U_{we}	U_{fe}	U_{we}	U_{fe}	U_{we}	U_{fe}	U_{we}	U_{fe}
	SPSW-100		SPSW-75		SPSW-50		SPSW-Opt	
10	5.3	10	5.5	13	5.7	16.5	6	22.1
9	5.3	10	5.6	13.3	5.8	14.2	6	17.3
8	5.4	9.5	5.6	11.6	5.9	14.8	5.8	14.7
7	5.5	10	5.7	11.9	5.9	13.1	5.9	15.6
6	5.6	9.2	5.7	10.6	5.9	13.2	5.9	14
5	5.6	9.4	5.8	11	5.9	13.3	6	14.5
4	5.6	8.5	5.8	9.9	6	13	5.9	13.7
3	5.6	8.5	5.9	10.1	6.1	13.6	6	13.5
2	5.7	7.7	5.8	9	6.2	12.1	6	13.4
1	6.3	9.3	6.4	10.6	6.6	13.7	6.5	15.1

* All dimensions are in mm.

3.2. Seismic evaluation of system

The major seismic parameters of the system, including ductility, response modification factor, over-strength factor, and energy absorption capacity of the frames, are calculated in this section and the effects of the design philosophy are investigated based on determining the actual contribution of the steel plate and frame to these parameters.

3.2.1. Ductility

According to ATC-24 [28], the displacement ductility factor of a system can be calculated using Eq. 9.

$$\mu = \frac{U_{\max}}{U_y} \tag{9}$$

Where μ is ductility factor, U_{max} is a maximum inelastic displacement that the system can experience before failure (supposed to be 0.02h in accordance with ASCE7-10 [27]), and U_y is the system's yield displacement.

The ductility of the frames in various stories is shown in Fig. 7. As can be seen, the less the plate's contribution to the story shear-capacity, the less the system's ductility would be. In other words, by reducing the plate's contribution from 100 % to the optimal value in different stories, the average ductility would be reduced from 8 to 6.3. According to Fig. 7, for every 25 % reduction in the plate's contribution relative to the SPSW-100 specimen, the system's ductility would be reduced by 9 %.

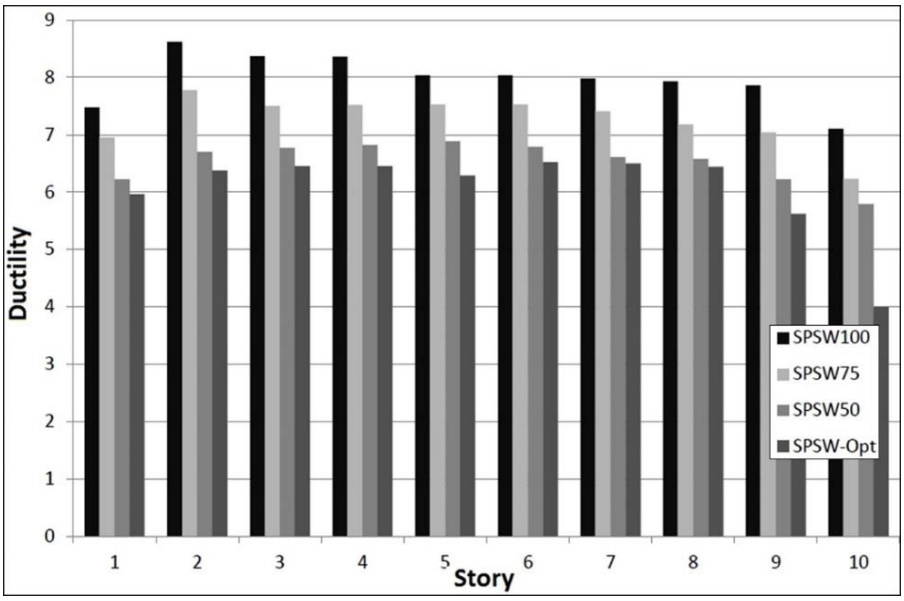

Figure 7. Ductility of the frames in different stories.

3.2.2. Energy absorption capacity

The area under the force-displacement diagram was equal to the system's energy absorption capacity [29]. In Fig. 8, the structure's energy absorption capacity on various stories for the studied specimens was calculated up to the displacement of 2 %.

The reduction in the steel plate's contribution to the story shear capacity led to the significant reduction of the system's energy absorption, which was mainly due to the reduction in the size of the peripheral frames as well as a reduction in the steel plate's thickness. In other words, the conventional overdesign (conservative) method would lead to a significant increase in the size of the columns and the thickness of the middle plate. It can be seen that in the optimal design, energy absorption capacity was less than the one in the conventional design, which does not mean the structure's inefficiency for earthquake energy absorption, and the energy absorbed by the system should be compared with the structural demand for various earthquakes. It should also be noted that the reduced frame dimensions and steel plate thickness would result in the reduced system stiffness and seismic demand. As previously mentioned, in this research, the designs were carried out by assuming the equal seismic requirements for the studied frames. According to Fig. 8, it can be seen that for every 25 % reduction in the plate's contribution relative to SPSW-100, the system's energy absorption capacity was reduced by 27 %.

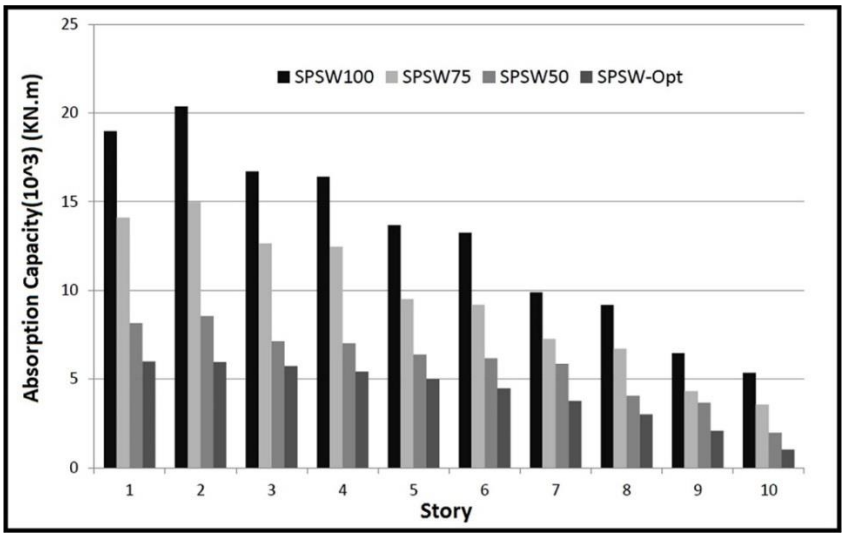

Figure 8. Energy absorption capacity of the frames in different stories.

3.2.3. Ductility reduction factor

One of the common methods to determine the reduction caused by ductility factor (R_μ) is Newmark and Hall method, which is calculated using Eq. 10. The median values of the periods (T) are calculated through interpolation [30].

$$\begin{aligned} T \le 0.03 \quad & R_\mu = 1 \\ 0.12 \le T \le 0.5 \quad & R_\mu = \sqrt{2\mu - 1} \\ T \ge 1 \quad & R_\mu = \mu \end{aligned} \tag{10}$$

Ductility reduction factors for the studied frames are shown in the second column of Table 4. It can be seen that by reducing the plate's contribution to the story shear, the ductility reduction factor would be also reduced. Therefore, the ductility reduction factor of the structure would be decreased by 6.8 on average for each 25 % reduction in the plate's contribution to the story shear.

Table 4. Seismic parameters of the frames.

Specimen	R_μ	Ω_0	R_u
SPSW-100	5.01	1.4	7.01
SPSW-75	4.67	1.5	7.01
SPSW-50	4.33	1.6	6.93
SPSW-Opt	4.2	1.65	6.94

3.2.4. Over-strength factor

Over-strength factor (Ω_0) is the strength that the structure demonstrates after forming the first plastic hinge (C_s) up to the mechanism (C_y), which is obtained using Eq. 11.

$$\Omega_0 = \frac{C_y}{C_s} \tag{11}$$

The over-strength factors were calculated for each story considering the PFI diagrams and, then, the average values were proposed on various stories of the studied frames in the third column of Table 4. It can be seen that by reducing the plate's contribution to the story shear capacity, the over-strength factor was increased so that, for every 25 % reduction in the plate's contribution to the story shear, the over-strength factor was increased by 7 %.

3.2.5. Response modification factor

Response modification factor in LRFD level was determined according to the following equation.

$$R_u = R_\mu \Omega_0 \tag{12}$$

Where R_u and Ω_0 indicate the ductility reduction and over-strength factors of the system. The mean values of the response modification factor on different stories of the studied frames are presented in the fourth column of Table 4. In this table, the behaviors of SPSW-100 and SPSW-75 were equal to 7.01, while for SPSW-50 and SPSW-Opt, they were 6.93 and 6.94, respectively. The interesting point about the mean values of the response modification factor in the studied frames was that, despite the reduction in the steel plate's contribution to the story shear capacity and the significant reduction in the size of the columns, beams, as well as the steel plate's thickness, the value of the computational response modification factor did not change significantly. In other words, the reduction in the value of the ductility reduction factor in the specimens with less contribution of the steel plate was compensated for by the increased over-strength factor of the structure.

3.3. Numerical study

Finite element analysis of the studied specimens was used to investigate the distribution of the forces in the steel wall and its peripheral frame at various drifts as well as the accuracy of the PFI diagrams and the obtained results.

For this purpose, ANSYS finite element software was used to model and investigate the specimens undergoing nonlinear static analysis (pushover). The thickness of the wall plate was very low in SPSW-50 and SPSW-Opt specimens. Furthermore, since the specimens were modeled with small computational thicknesses and actual dimensions of the frames in the software, the lateral deformations of plate were relatively too high. Therefore, it was so difficult to converge the models. In addition, due to the huge volume of the calculations in modeling a 10-storey structure in software, only the first two stories were modeled for two SPSW-100 and SPSW-75 specimens in the software in order to investigate the shear behavior of the first story. It was necessary to model the second story to investigate the correct beam role for the tensile force of the lower and upper stories due to tension field in steel walls. Therefore, the two-story model was used for studying the ground story.

3.3.1. Finite element modeling

The steel wall and frame elements were selected by SHELL181 element type, which included 4 nodes with 3 degrees of transitional freedom as well as 3 degrees of rotational freedom. Besides, it was capable of modeling large buckling deformations. The column base-to-ground connection, plate-to-beam and column connection, as well as beam-to-column connections were continuous. The out-of-plane deformation of the frame was prevented. The S350J steel materials with the minimum yield strength of 350 MPa were used for the beams and columns and S235J steel with the minimum yield strength of 235 MPa were used for the steel wall. The reason for using the steel with higher yield stress for the peripheral frame was to reduce the size of columns and beams to the minimum possible dimensions. Materials were considered bilinear with the strain-hardening slope of 1 % and the optimum mesh size was considered equal to 200 mm. Fig. 9 shows the two-story model built in software. As demonstrated in this figure, due to the use of RBS in the beam-column connection, meshing at the end of the beam and also at the points adjacent to the columns was finer. Moreover, in order to prevent the concentration of the stresses in the panel zone, the continuity plates were used in the columns.

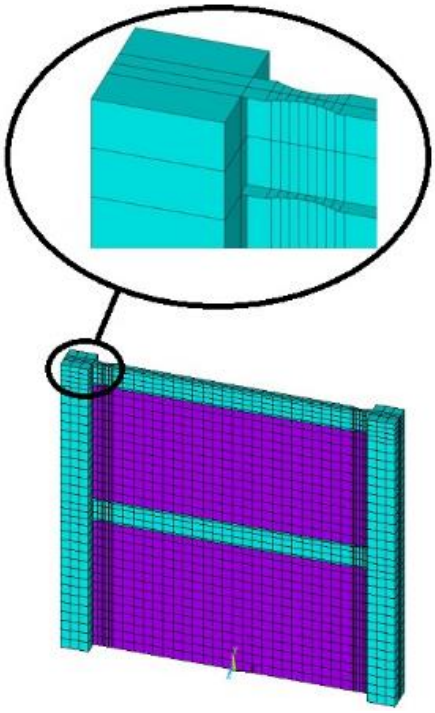

Figure 9. Finite element model.

3.3.2. Force-displacement diagrams

The force-displacement curves of the software models and the PFI diagrams of the studied specimen are compared in Fig. 10. As can be seen, the diagrams obtained from the software were compatible with PFI diagrams.

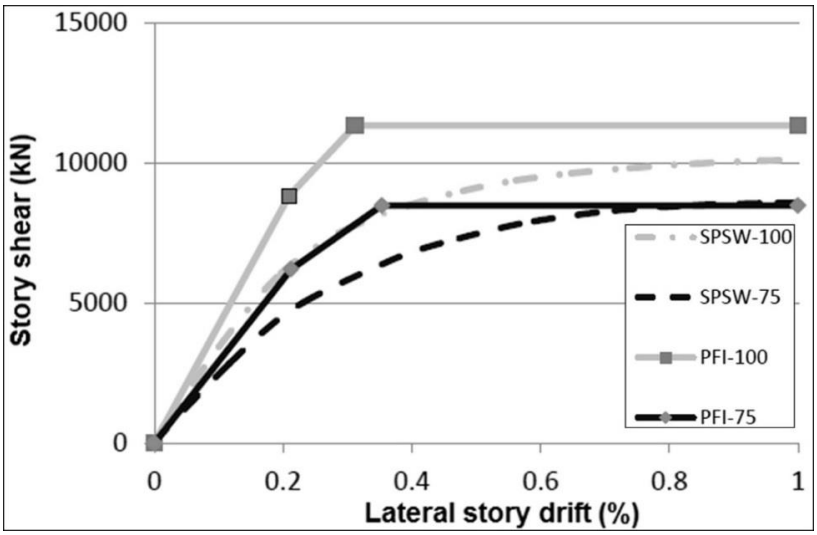

Figure 10. Comparing software and PFI pushover diagrams.

3.3.3. Stress distribution in steel wall

Fig. 11 and 12 represent the distribution and the values of stresses (in MPa) inside the steel wall at different drifts. As shown in these figures, the stresses began to increase from the corner of the plate toward center. A larger area of the plate was yielded by increasing the lateral story drift. Finally, a major part of the wall was yielded at 1 % drift in SPSW-100 and SPSW-75 specimens.

First yield point of the plate in SPSW-100 occurred at 0.13 % drift, while the yield point in the SPSW-75 was at 0.09 % drift. In other words, the reduction in the contribution of the steel wall led to smaller drifts for the first yield of the steel plate. For example, the total yield point of the wall in SPSW-100 occurred at the displacement of 4.3 mm, while the yield point in SPSW-75 was at the displacement of equal to 5 mm.

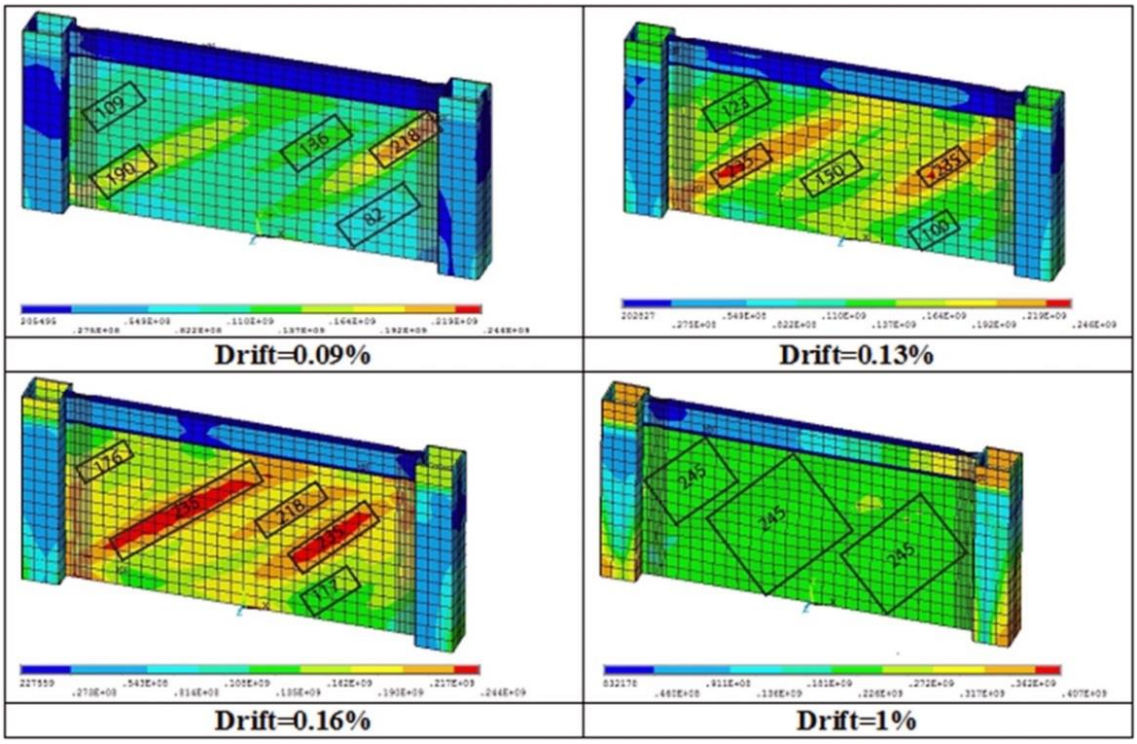

Figure 11. Von-Mises stress distribution in various drifts in SPSW-100.

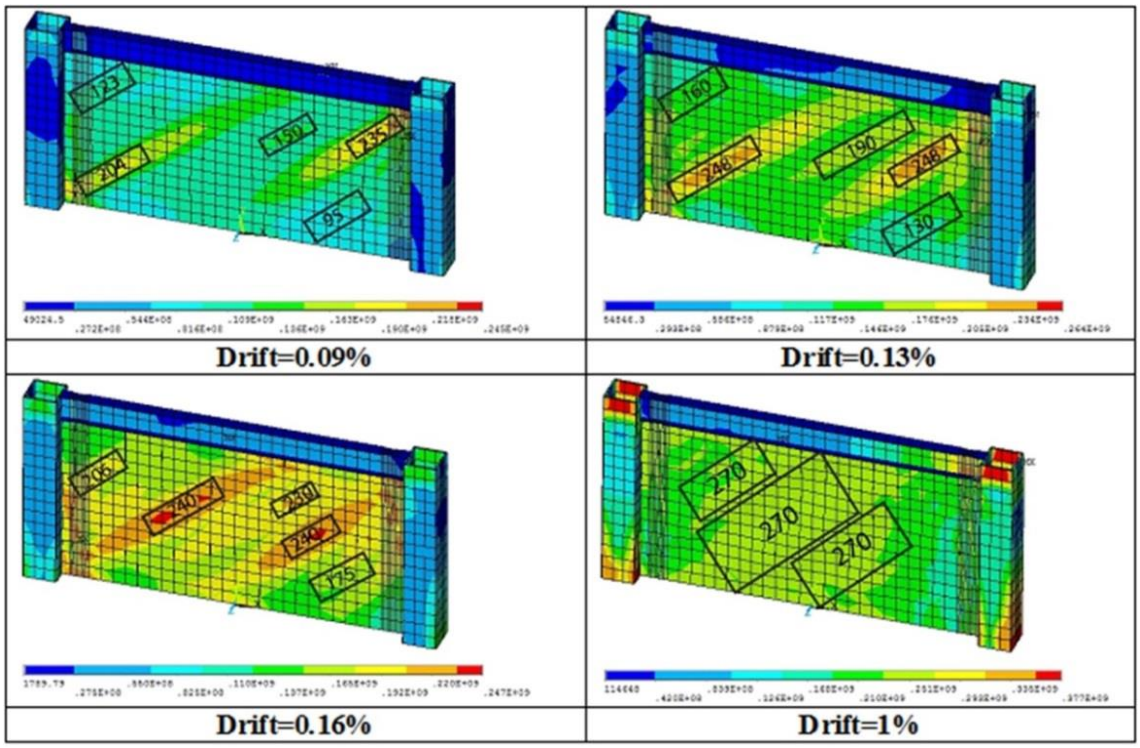

Figure 12. Von-Mises stress distribution in various drifts in SPSW-75.

3.3.4. Behavior of RBS connection

In order to follow the strong column-weak beam philosophy in accordance with AISC358 [31] requirements, the RBSs were provided at the ends of beams.

The Von-Mises stress distribution in RBS connections at various drifts is shown in Fig. 13. The average stress values are written on the figure. The use of RBS led to the increased stress in the reduced area, formation of plastic hinges in the beams, as well as prevention of the formation of the plastic hinge in the columns. It can be seen that the first yield point of the RBS connection was occurring at 0.4 % drift, which protected the column against unfavorable effects of stress concentration adjacent columns' face.

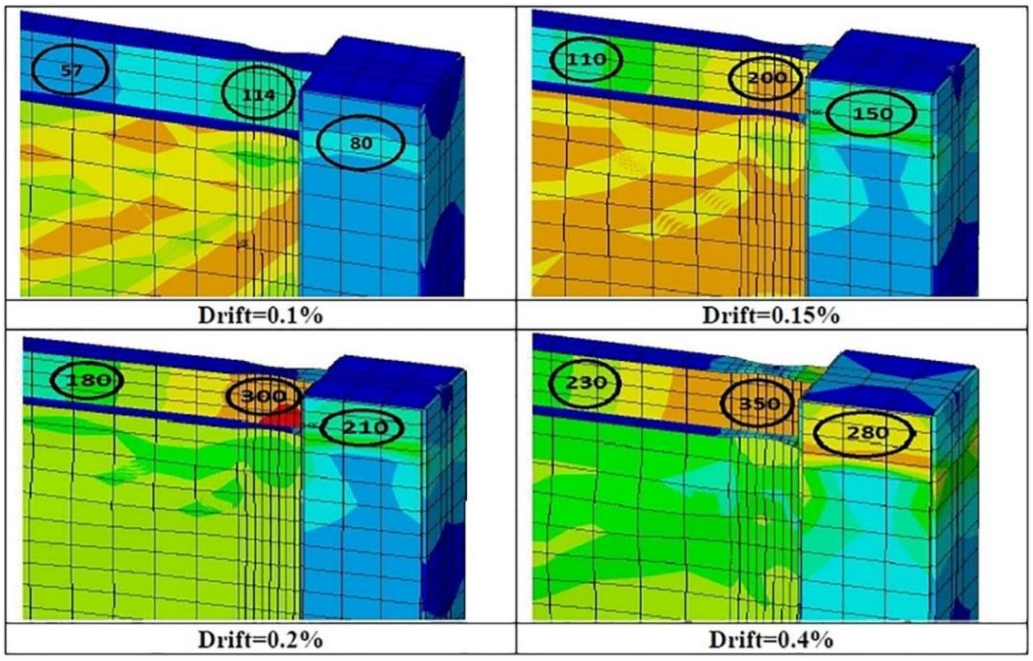

Figure 13. Von-Mises stress distribution in RBS connections at various drifts.

3.3.5. Out-of-plane displacements of steel wall

The out-of-plane deflections of steel wall is shown in Fig. 14. In SPSW-100, the thickness of the steel plate on the first story was 5.8 mm, where the maximum out-of-plane displacement at 1 % drift was 40 mm. In SPSW-75, the thickness of the steel plate on the first story was 4.3 mm, while the maximum displacement at 1 % drift was 36.5 mm. It is observed that, despite the considerable reduction in the steel plate's thickness in SPSW-75 compared to SPSW-100, the value of the out-of-plane deformation of the plate did not change significantly. In other words, by reducing the wall's contribution to the lateral load transfer, the number of the out-of-plane deformation waves of the plate (number of protrusions and indentations of the plate) was increased, while the maximum displacement value along the out-of-plane direction of the steel plate was reduced.

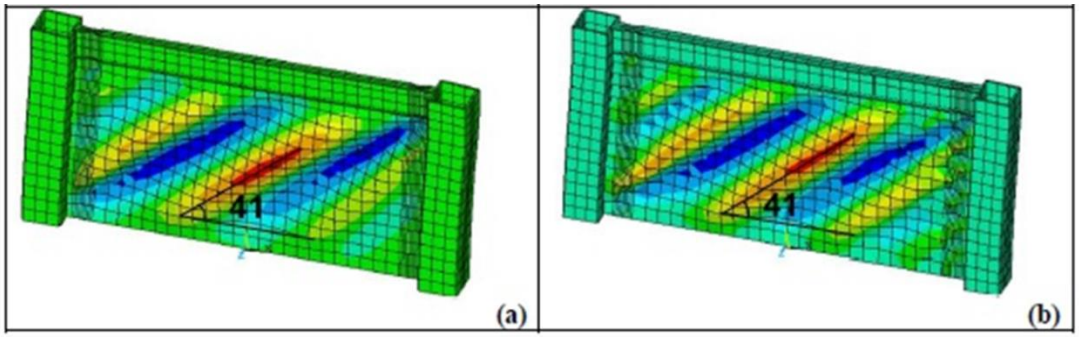

Figure 14. Out-of-plane deflection of steel wall in 1 % drift, a) SPSW-100, b) SPSW-75.

3.3.6. Tension field angle

As shown in Fig. 14, the diagonal tension field angles in both SPSW-100 and SPSW-75 were 41°. Therefore, by decreasing the plate's contribution to the lateral load transfer, the value of the tension field angle did not change significantly.

3.3.7. Contribution of steel plate and peripheral frame in the story shear

To determine the value of transferring shear by the steel wall and its peripheral frame, the value of horizontal forces of the wall at the wall's node connection to the foundation at various drifts was added and the remaining shear was tolerated by the peripheral frame (see Fig. 15).

According to Fig. 15, by increasing the structure's drift, the contribution of the steel plate to the story's shear transfer was reduced. Furthermore, the contribution of the plate in SPSW-75 was more. Therefore, in SPSW-100, the steel plate and its peripheral frame transferred about 54 % and 46 % of the total story's shear

at the beginning of loading, respectively, while at 1 % drift, the steel plate and its peripheral frame transferred about 38 % and 62 % of the shear, respectively. In SPSW-75, the steel plate and its peripheral frame transferred about 54 % and 46 % of the total story's shear (similar to SPSW-100), respectively, while at 1 % drift, the steel plate and its peripheral frame transferred about 33 % and 67 % of the story's shear, respectively. In other words, by increasing the structure's drift, the contribution of the steel wall to the story's shear capacity in SPSW-75 was decreased much more than the one in SPSW-100. It should be noted that in designing SPSW-100, the total story shear was allocated to the steel wall, while the contribution of the steel wall varied only between 38 % and 54 %. Similarly, in SPSW-75, in which the steel wall was designed to transfer 75 % of the total story shear, the contribution of the steel wall was between 33 % and 54 % of the system's total capacity. The diagrams indicated that the shear percentage allocated for designing the steel walls was over-estimated and, in practice, the walls had less contribution in story shear. Furthermore, a large amount of the story shear was transmitted by columns and neglecting the role of peripheral frame in the story shear would lead to the non-economic design of the SPSW system.

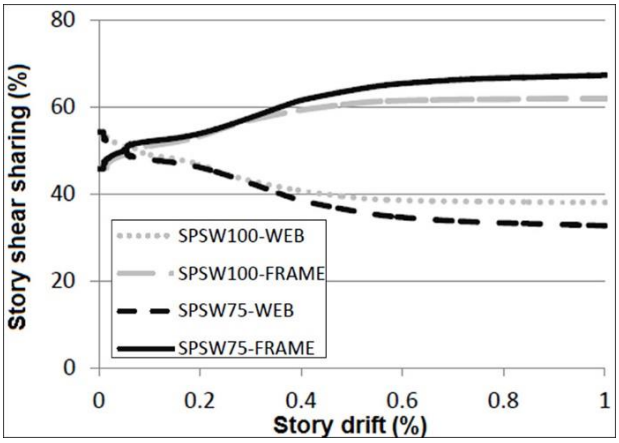

Figure 15. Contribution of steel plate and peripheral frame in the story shear versus drift.

4. Conclusion

Four specimens of steel shear wall in a 10-story building were designed for 100, 75, 50 %, and the optimal percentage of shear transfer and the capacity of each frame was compared with the demand shear capacity of each story. According to the results, designing the wall for higher shear percentage and neglecting the role of columns in the story shear capacity would increase the frame's thickness and the peripheral frame dimensions, leading to the non-economic system. Furthermore, according to the PFI diagrams and finite element modeling of the specimens, in the specimens with less contribution of the steel plate to the story shear, the value of the ductility reduction factor was decreased and the structure over-strength factor was increased, while the mean value of the structure's response modification factor did not change significantly. In general, it can be concluded that by determining the precise contribution of the steel plate and its peripheral frame for the earthquake demand story shear, it would be possible to design SPSW for more optimized sections.

Finite element analysis of the studied specimens also indicated much less contribution of the steel plate to the story shear. In order to complete the discussions presented in this research, it is necessary to conduct further studies on the structures with different numbers of stories as well as on the behavior of the structures under nonlinear time history analysis and incremental dynamic analysis (IDA). Moreover, providing an optimal design requires further studies in this regard. In addition, the accurate definition of earthquake demands considering the reduced stiffness of the system and decreased base shear may result in more optimized system.

5. Acknowledgments

The research described in this paper was supported by Shahr-e-Qods Branch of Islamic Azad University.

References

1. Roberts, T.M., Sabouri-Ghomi, S. Hystertic Characteristics of Unstiffened Plate Shear Panels. Thin Walled Structures, 1991. 12(2). Pp. 145–162.
2. Sabouri-Ghomi, S., Ventura, C.E., Kharrazi, M.H.K. Shear Analysis and Design of Ductile Steel Plate Walls. Journal of Structural Engineering, ASCE, 2005. 131(6). Pp. 878–889.

3. Gholhaki, M. Investigating behavior of ductile steel shear walls and effect of type of beam-column joint. Ph.D. thesis, Department of Civil and Environmental Engineering, K.N. Tousi University of Technology, 2008.
4. Darvishi, A., Jamshidi, M., Qaffari, H., Mir-Babaei, S.A. Investigating effect of column's stiffness on load bearing capacity of steel shear walls, National Conference on Structure-Road-Architecture, Islamic Azad University, Chalous Branch, Chalous-Iran, 2011.
5. Alinia, M.M., Dastfan, M. The Effects of Surrounding Members on Post-Buckling Behavior of Thin Steel Plate Shear Walls (TSPSW). Advances in Steel Structures, Elsevier Ltd, 2005. 2. Pp. 1427–1432.
6. Alinia, M.M., Dastfan, M. Behavior of Thin Steel Plate Shear Walls Regarding Frame Members. Journal of Constructional Steel Research, 2006. 62(7). Pp. 730–738.
7. Alinia, M.M., Dastfan, M. Cyclic Behavior, Deformability and Rigidity of Stiffened Steel Shear Panels. Journal of Constructional Steel Research, 2007. 63(4). Pp. 554–563.
8. Choi, L., Park, H. Cyclic Test for Framed Steel Plate Walls with Various Infill Plate Details. Proceedings, the 14th World Conference in Earthquake Engineering, Beijing-China, 2008.
9. Kharrazi, M.H., Ventura, C.E., Prion, H.G. Analysis and Design of Steel Plate Walls: Analytical Model. Canadian Journal of Civil Engineering, 2010. 38(1). Pp. 49–59.
10. Chen, S.h., Jhang, C.h. Experimental Study of Low-Yield-Point Steel Plate Shear Wall Under in-Plane Load. Journal of Construction Steel Research, 2011. 67. Pp. 977–985.
11. Hosseinzadeh, S.A.A., Tehranizadeh, M. Behavioral Characteristics of Code Designed Steel Plate Shear Wall Systems. Journal of Construction Steel Research, 2014. 99. Pp. 72–84.
12. Moradinejad, Z., Gholampour, S., Vaseghi Amiri, J. Investigating effect of position of steel shear wall on progressive failure using nonlinear static analysis. 6th National Congress on Structure and Steel, Tehran-Iran, 2014.
13. Ebadi, P., Farajloomanesh, S., Pishbin, M. Required ductility and capacity for designing steel buildings with special steel shear wall system without stiffener, International Conference on Architecture – Civil Engineering and Urban Planning in 3rd Millennium, Tehran-Iran, 2014.
14. Ebadi, P., Farajloomanesh, S., Pishbin, M. Effect of plate's contribution to shear tolerance of story in special steel shear wall system without stiffener. 6th National Conference on Structure and Steel, Tehran-Iran, 2014.
15. Purba, R., Bruneau, M. Experimental investigation of steel plate shear walls with in-span plastification along horizontal boundary elements. Engineering Structures, 2015. 97. Pp. 68–79.
16. Moghimi, H., Driver, R.G. Performance assessment of steel plate shear walls under accidental blast loads. Journal of Constructional Steel Research, 2015. 106. Pp. 44–56.
17. Guo, H.C., Hao, J.P., Liu, Y.H. Behavior of stiffened and unstiffened steel plate shear walls considering joint properties. Thin-Walled Structures, 2015. 97. Pp. 53–62.
18. Du, Y., Hao, J., Yu, J., Yu, H., Deng, B., Lv, D., Liang, Z. Seismic performance of a repaired thin steel plate shear wall structure. Journal of Constructional Steel Research, 2018. 151. Pp. 194–203.
19. Wang, W., Ren, Y., Lu, Z., Song, J., Han, B., Zhou, Y. Experimental study of the hysteretic behaviour of corrugated steel plate shear walls and steel plate reinforced concrete composite shear walls. Journal of Constructional Steel Research, 2019. 160. Pp. 136–152.
20. Jalali, S.A., Darvishan, E. Seismic demand assessment of self-centering steel plate shear walls. Journal of Constructional Steel Research, 2019. 162. P. 105738.
21. Yu, J.G., Liu, L.M., Li, B., Hao, J.P., Gao, X., Feng, X.T. Comparative study of steel plate shear walls with different types of unbonded stiffeners. Journal of Constructional Steel Research, 2019. 159. Pp. 384–396.
22. Pachideh, G., Gholhaki, M., Daryan, A.S. August. Analyzing the damage index of steel plate shear walls using pushover analysis. In Structures-Elsevier, 2019. 20. Pp. 437–451.
23. Hajimirsadeghi, M., Mirtaheri, M., Zandi, A.P., Hariri-Ardebili, M.A. Experimental cyclic test and failure modes of a full scale enhanced modular steel plate shear wall. Engineering Failure Analysis, 2019. 95. Pp. 283–288.
24. Mu, Z., Yang, Y. Experimental and numerical study on seismic behavior of obliquely stiffened steel plate shear walls with openings. Thin-Walled Structures, 2020. 146. P. 106457.
25. ANSI/AISC 341, Seismic Provisions for Structural Steel Buildings. American Institute of Steel Construction, 2005.
26. AISC Steel Design Guide 20, Steel Plate Shear Walls. American Institute of Steel Construction, 2007.
27. ASCE/SEI 7-10, Minimum Design Loads for Buildings and Other Structures. American Society of Civil Engineering, 2010.
28. ATC-24, Guidelines for Seismic Testing of Components of Steel Structures. Report-24, Applied Technology Council, 1992.
29. ATC-40, Seismic evaluation and retrofit of concrete buildings. Applied Technology Council, 1996.
30. Borzi, B., Elnashai, A.S. Refined force reduction factors for seismic design Engineering Structures, 1991. 22. Pp. 1244–1260.
31. ANSI/AISC 358-10, Prequalified Connections for Special and Intermediate Steel Moment Frames for Seismic Applications. American Institute of steel construction Inc., 2010.

Contacts:

Parviz Ebadi, parviz.ebadi@gmail.com

Saeid Farajloomanesh, s.farajloomanesh@gmail.com